BIOCHEMISTRY
including biophysical chemistry & molecular biology
Article

Biochemistry **2011,** *50,* 1763–1770 1763
DOI: 10.1021/bi101789y

Inhibition Mechanism of Rat $\alpha_3\beta_4$ Nicotinic Acetylcholine Receptor by the Alzheimer Therapeutic Tacrine†

Arquimedes Cheffer and Henning Ulrich*

Departamento de Bioquímica, Instituto de Química, Universidade de São Paulo, São Paulo 05508-900, Brazil

Received November 8, 2010; Revised Manuscript Received January 18, 2011

ABSTRACT: Nicotinic acetylcholine receptors (nAChRs) were studied in detail in the past regarding their interaction with therapeutic and drug addiction related compounds. Using fast kinetic whole-cell recording, we have now studied effects of tacrine, an agent used clinically to treat Alzheimer's disease, on currents elicited by activation of rat $\alpha_3\beta_4$ nAChR heterologously expressed in KXα3β4R2 cells. Characterization of receptor activation by nicotine used as agonist revealed a K_d of 23 ± 0.2 μM and 4.3 ± 1.3 for the channel opening equilibrium constant, Φ^{-1}. Experiments were performed to investigate whether tacrine is able to activate the $\alpha_3\beta_4$ nAChR. Tacrine did not activate whole-cell currents in KXα3β4R2 cells but inhibited receptor activity at submicromolar concentration. Dose−response curves obtained with increasing agonist or inhibitor concentration revealed competitive inhibition of nAChRs by tacrine, with an apparent inhibition constant, K_I, of 0.8 μM. The increase of Φ^{-1} in the presence of tacrine suggests that the drug stabilizes a nonconducting open channel form of the receptor. Binding studies with TCP and MK-801 ruled out tacrine binding to common allosteric sites of the receptor. Our study suggests a novel mechanism for action of tacrine on nAChRs besides inhibition of acetylcholine esterase.

The tobacco alkaloid nicotine exerts its effects on the central and peripheral nervous system (CNS and PNS) through ligand-gated ion channels, named nicotinic acetylcholine receptors. To date, 11 neuronal (α2−α7, α9−α10, β2−β4) and 5 muscular (α1, β1, γ, ε, δ) nAChR[1] subunit genes have been identified in the mammalian genome. The nAChRs can assemble from five copies of a single type of subunit, but they more commonly assemble from several different types of subunit, giving raise to a relatively hydrophilic way and allowing the influx of cations such as Na^+, K^+, and Ca^{2+} (*1*). These receptors are involved at a wide range of physiological and pathophysiological processes. They are located in the neuromuscular junction, where they play a key role in creating the skeletal muscle tone and, in the CNS, where they are involved in several processes related to cognitive functions, learning and memory, motor control, and analgesia (*2*).

Several compounds target nAChRs and inhibit them by allosteric mechanisms or by competition for agonist binding sites, i.e., α-bungarotoxin. Noncompetitive, allosteric inhibition was observed for local anesthetics such as procaine and QX-222 (*3*, *4*), the anticonvulsant dizocilpine (MK-801) (*5*), tenocyclidine (TCP, thienylcyclohexylpiperidine), and the abused drugs phencyclidine (PCP) and cocaine (*6*) as well as for cembranoids isolated from sea anemones and tobacco (Figure 1) (*7*, *8*).

One of the most prominent expressed subtypes of neuronal nAChRs is the $\alpha_3\beta_4$ one, expressed in autonomic ganglia, controlling the release of the catecholamines norepinephrine and epinephrine. These receptors are also present in particularly high density in the superior cervical ganglion, pineal and adrenal glands, *substantia nigra*, striatum, hippocampus, *locus coeruleus*, habenulointerpeduncular tract, and cerebellum (*9*). Receptor inhibition by anesthetics (barbiturates, etomidate, and propofol, for example) has been reported and can explain, up to a certain point, arterial hypotension observed during anesthesia (*10*). At the same time, $\alpha_3\beta_4$ nAChR inhibition attenuated the signs of opioid withdrawal (*11*).

Tacrine used for the treatment of Alzheimer's disease (AD) inhibits acetylcholine esterase (AChE) and protects acetylcholine from degradation, increasing cholinergic neurotransmission aiming at counteracting the disease state which is characterized by the loss of cholinergic neurons and nAChRs throughout the brain (*12*). However, experimental evidence points at direct action of tacrine with neuronal nAChRs (*13*, *14*). Here we show that tacrine inhibits nicotine-evoked $\alpha_3\beta_4$ nAChR activity by a competitive mechanism. A rapid chemical technique with a time resolution of 10 ms (*15*) was used to obtain kinetic parameters and compare them with those observed with the noncompetitive nAChR inhibitor MK-801.

MATERIALS AND METHODS

Materials. Unless otherwise indicated, all reagents were purchased from Sigma and were of the highest available quality. [^{3}H]TCP (40.8 Ci/mmol) was purchased from PerkinElmer (Fremont, CA, USA).

Cell Culture and Maintenance. KXα3β4R2 cells expressing recombinant rat $\alpha_3\beta_4$ receptors (*16*) were grown in Dulbecco's modified Eagle's medium (DMEM, high glucose; Invitrogen) supplemented with 10% (v/v) fetal bovine serum (Cultilab, Campinas, Brazil) in the presence of 100 IU/mL penicillin, 100 μg/mL streptomycin, and 0.7 mg/mL Geneticin at 37 °C in a

†This work was supported by research grants from Fundação de Amparo à Pesquisa do Estado de São Paulo (FAPESP) and Conselho Nacional de Desenvolvimento Cientifico (CNPq), Brazil, awarded to H. U. A.C. graduate studies research is supported by a fellowship from FAPESP.

*To whom correspondence should be addressed. E-mail: henning@iq.usp.br. Telephone: +55-11-3091-3810 ext 223. Fax: +55-11-3815-5579.

[1]Abbreviations: nAChR, nicotinic acetylcholine receptor; AChE, acetylcholine esterase; AD, Alzheimer's disease.

Published on Web 01/19/2011

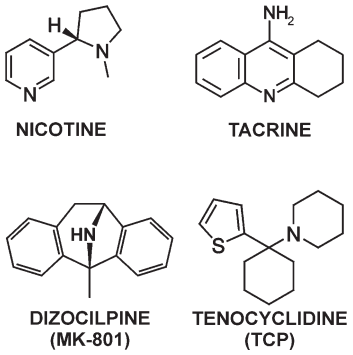

FIGURE 1: Molecular structures of nicotine, tacrine, MK-801, and TCP. Nicotine and tacrine potentiate cholinergic neurotransmission, the former functioning as agonist and directly activating the nAChRs, and the latter inhibiting acetylcholinesterase (AChE). MK-801 and TCP are well-known nAChR inhibitors. TCP is a structural analogue of the abused drug phencyclidine.

water-saturated atmosphere containing 5% CO_2. Cell cultures were seeded at a density of 5×10^5 cells/culture flask (175 cm^2) (Cultilab, Campinas, Brazil) and subcultured weekly. Cells were fed three times during that period by replacing the old medium. For electrophysiology, 2×10^4 cells were plated into 35 mm cell culture dishes and used for experiments within 2−4 days.

Whole-Cell Current Recording. Recording glass pipets were pulled from borosilicate glass (World Precision Instruments Inc., Berlin, Germany), using a two-stage puller (Sutter P-0; Sutter Instruments, Novato, CA). Pipet tips were fire-polished using a flame polisher (MF-83; Narishige, Tokyo, Japan). The extracellular recording buffer contained 145 mM NaCl, 5.3 mM KCl, 1.8 mM $CaCl_2 \cdot 2H_2O$, 1.2 mM $MgCl_2$, 10 mM glucose, and 10 mM HEPES, pH 7.4. The intracellular solution consisted of 140 mM KCl, 10 mM NaCl, 2 mM $MgCl_2$, 1 mM EGTA, and 10 mM HEPES, pH 7.4. An Axopatch 200A amplifier and the pClamp software packet (Molecular Devices Corp., Union City, CA) were used for data collection. The obtained data were analyzed on a personal computer using Microcal Origin (Northampton, MA). All measurements were carried out at a transmembrane voltage of −70 mV. Data from each cell were normalized to the response measured with 300 μM nicotine. All solutions used in the experiments were prepared on the day of the measurement.

Rapid Application of Ligand Solution. The flow method used for rapid ligand application has been described by Krishtal and Pidoplichko (*15*) and Udgaonkar and Hess (*17*). Briefly, a cell in the whole-cell recording configuration (*18*) was placed ca. 100 μm from the porthole (diameter of ca. 100 μm) of a U-tube (Hamilton, Reno, NV) (*15*). The flow rate of solutions emerging from the flow device, containing neurotransmitter with or without inhibitor, was typically 1 cm/s. The observed rise time of the whole-cell current to its maximum value, characteristic of the time for nicotine to equilibrate with the cell surface receptors, was 10−15 ms. The cells were allowed to recover for 3 min between each experiment, a time sufficient to guarantee full recovery of the receptors from desensitization.

Current Correction for Desensitization in Cell-Flow Measurements. The current maximum amplitude is a measurement of the concentration of open-receptor channels. In cell-flow experiments, the observed maximum current amplitude was corrected for the rate of desensitization occurring while the receptors equilibrate with the channel-activating solution that flows over the cell surface (*17*, *18*). This correction was performed using eq 1 and provides the maximum current amplitude corrected for the desensitization (I_A).

$$I_A(t_n) = (e^{\alpha \Delta T} - 1) \sum_{i=1}^{n} (I_{obs})_{\Delta t_i} + (I_{obs})_{\Delta t_n} \quad (1)$$

in which $(I_{obs})_{\Delta t_i}$ is the observed current during the ith time interval. $I_A(t_n)$ becomes equal to I_A when the t_n value is either equal to or longer than the time it takes for the current to reach its maximum amplitude.

Data Analysis. Data analysis was performed under the condition that the agonist (in this case, nicotine) needs to interact with two binding sites of the receptor for channel opening and that agonist binding to both sites with the same affinity (*19*), as shown by the scheme:

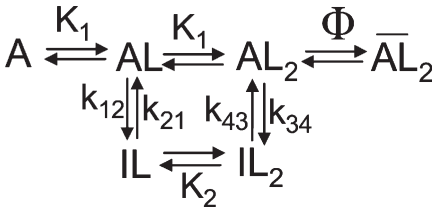

A represents the active, nondesensitized receptor; the subscripted number 2 indicates the number of agonist molecules bound. $\overline{AL}_2$ is the open-channel form of the receptor, and I denotes the inactive desensitized form of the receptor. K_1 and K_2 are dissociation constants for agonist binding to nondesensitized and desensitized receptors, respectively. The rate constants k describe the desensitization process and Φ describes the channel-closing equilibrium constant.

Dose−Response Curve. The EC_{50} and n_H values were calculated by linear regression using the GraphPad Prism software (San Diego, CA). K_1 was determined using eq 2 (*20*):

$$I_A = \frac{I_{max}}{\left[\frac{K_1}{L} + 1\right]^2 \Phi + 1} \quad (2)$$

I_{max} represents the maximum current obtained from one cell when all receptor channels are open; K_1 is the agonist dissociation constant; L is the agonist concentration; Φ is the channel-closing equilibrium constant, and I_A are the current amplitudes obtained experimentally and corrected for desensitization. This equation is linearized (eq 3):

$$\left(\frac{I_{max}}{I_A} + 1\right)^{1/2} = \Phi^{1/2} + \frac{K_1}{L} \Phi^{1/2} \quad (3)$$

Dose−Response Curve in the Presence of a Competitive Inhibitor.

$$\left(\frac{I_{max}}{I_A} + 1\right)^{1/2} = \Phi^{1/2}\left(1 + \frac{K_1}{L}\right) + \frac{IK_1}{K_I L} \Phi^{1/2} \quad (4)$$

I is the inhibitor concentration, and K_I is its inhibition constant. The other constants were already defined before. This equation was used to analyze how the current measurements vary with the inhibitor concentration. The inhibition constant (K_I) describes the affinity of the inhibitor for the receptor and can be determined

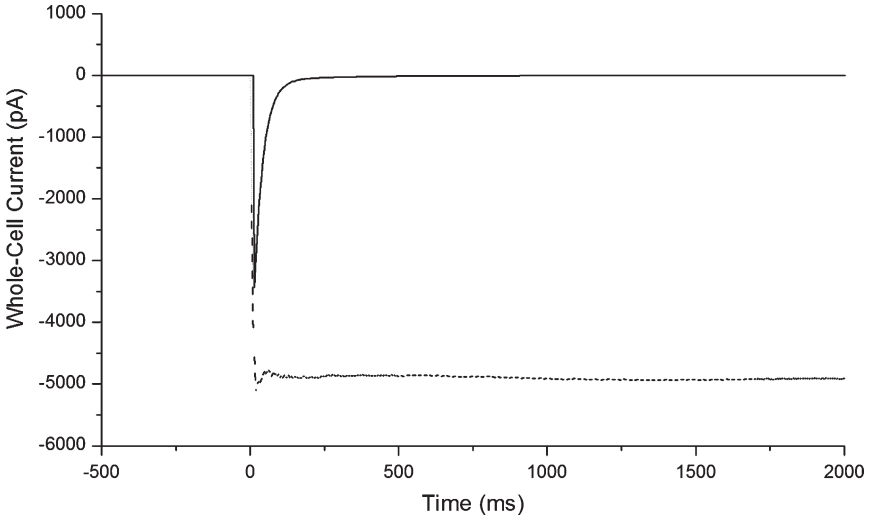

FIGURE 2: Whole-cell current response evoked by $\alpha_3\beta_4$ nAChR activation in the presence of 1 mM nicotine. Measurements were carried out with KXα3β4R2 cells at pH 7.4, room temperature, and a transmembrane voltage of −70 mV with a flow rate of the nicotine solution of ~1 cm/s for the rapid equilibration of cell surface receptor with the ligand. The observed whole-cell current (solid line) is a measure of the number of receptors in the open-channel form in the cell membrane. The falling phase of the current, indicative for receptor desensitization, reveals two processes: ~98% of the current decays with a rate coefficient of 9.5 s^{-1}, and ~2% of the current decays with a rate coefficient of 0.1 s^{-1}. The dotted line parallel to the time axis represents the current corrected for the rate of desensitization that occurs during the rising phase of the current (*17*) (eq 1).

by using eq 5:

$$K_I = \frac{IC_{50}}{1+\frac{L}{EC_{50}}} \quad (5)$$

assuming that inhibitor and ligand (agonist) bind to the same site of the receptor (*21*). The IC_{50} was determined using a Hill fitting.

Noncompetitive Inhibition.

$$\left(\frac{I_{max}}{I_A}-1\right)^{1/2} = \left(\Phi^{1/2}+\frac{K_1}{L}\Phi^{1/2}\right)Z \quad (6)$$

where $Z = (I/K_1)(1/1 - F\overline{AL_2})^{1/2}$ when the noncompetitive inhibitor I binds to all forms of the receptor and $Z = (I/K_I + 1)^{1/2}$ when the noncompetitive inhibitor binds only to the closed-channel forms of the receptor.

General Noncompetitive Inhibition.

$$\frac{I_A}{I_{A(I)}} = 1+\frac{I}{K_I} \quad (7)$$

I is the concentration of the noncompetitive inhibitor, and K_I is the inhibition constant. I_A and $I_{A(I)}$ are the obtained currents at a constant agonist concentration in the presence and in the absence of inhibitor, respectively.

Competitive Inhibition.

$$\frac{I_A}{I_{A(I)}} = 1+\frac{I}{K_I}\left[(2F_A+F_{AL})+F_A\frac{I}{K_I}\right] \quad (8)$$

I is the concentration of the inhibitor, and K_I is its inhibition constant. F_A and F_{AL} are the fractions of unoccupied receptors and receptor species bound to one ligand molecule at equilibrium, respectively:

$$F_A = \frac{\left(\frac{K_1}{L}\right)^2\Phi}{\left(\frac{K_1}{L+1}\right)^2\Phi+1} \quad F_{AL} = \frac{2\left(\frac{K_1}{L}\right)\Phi}{\left(\frac{K_1}{L}+1\right)^2\Phi+1}$$

It is noteworthy that, when the term $F_A(I/K_I) \ll 2F_A + F_{AL}$, that is, at low inhibitor concentrations, the equation for competitive inhibitor reduces to that one for noncompetitive inhibitors (*22*).

Binding of [^{3}H]TCP to $\alpha_3\beta_4$ nAChRs. For binding measurements, 1.75×10^4 KXα3β4R2 cells were plated into 24-well plates and used for experiments within 2 days. The cells were incubated for 40 min with 19.6 nM [^{3}H]TCP (40.8 Ci/mmol) in the absence or presence of increasing concentrations of competitors MK-801 and tacrine (100 pM−1 mM) in a total volume of 200 μL of extracellular buffer. Then cells were washed three times with 200 μL of extracellular buffer and were then solubilized in 1% SDS. The radioactivity retained by the cell layer was determined by liquid scintillation counting. MK-801, a noncompetitive inhibitor of $\alpha_3\beta_4$ nAChRs, was used in control experiments. The affinities of the ligands to their binding sites on the receptors were registered as IC_{50} values, the concentration at which the ligands displace 50% of the radioactive ligand from the receptor (*6*).

Statistical Analysis. The experimental data were analyzed by using the unpaired Student's t test, in which differences were considered statistically significant when p values were smaller than 0.05. Data were expressed as mean values ± standard deviation.

RESULTS

Agonist-Induced Effects. Whole-cell current measurements in combination with fast kinetic ligand application, the cell flow technique, were done with a KXα3β4R2 cell in the presence of 1 mM nicotine (Figure 2). The maximal response was obtained within 10−15 ms, then decaying in agreement with a two exponential process. The rate coefficients for fast and slow receptor desensitization, α and β, were calculated to be 9.5 and 0.1 s^{-1}, respectively, indicating that the initial desensitization process occurs around 120 times faster than the second one. Similarly, the receptor fraction that desensitizes quickly is far greater (98%) than the receptor fraction related to the slow desensitization process (2%). This second process, therefore, was not taken into account for data analysis. The current corrected for desensitization that takes place during the equilibration of nicotine with the

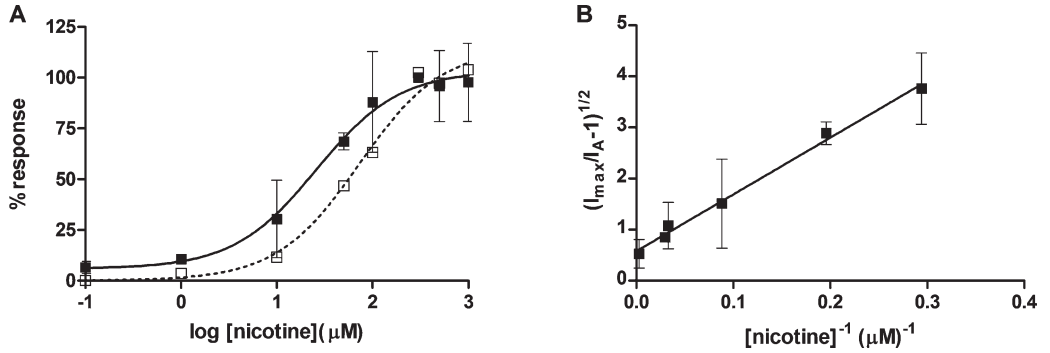

FIGURE 3: Dose-dependent activation of $\alpha_3\beta_4$ nAChRs by nicotine in the absence and presence of 20 μM tacrine. Whole-cell currents collected at various nicotine concentrations were normalized to average responses obtained in the presence of 300 μM nicotine which was considered as 100% response. Current amplitudes were corrected for receptor desensitization as detailed in the Materials and Methods section. Three to nine measurements from a total of 10 cells were made at each concentration of nicotine. (A) Data were fitted to eq 1. The EC_{50} was determined as 22 ± 4 μM ($R^2 = 0.99$) with a Hill coefficient of 1 ± 0.2. For comparison, the dependence of the response on the concentration of nicotine in the presence of 20 μM tacrine (dashed line and open squares) is also shown. (B) Data were fitted to the linear form of eq 2 with a slope of 11.03 ± 2.89 and an intercept of 0.48 ± 0.14, providing values for the channel-opening equilibrium constant Φ^{-1} and K_I of 4.3 ± 1.3 and 23 ± 0.2 μM, respectively.

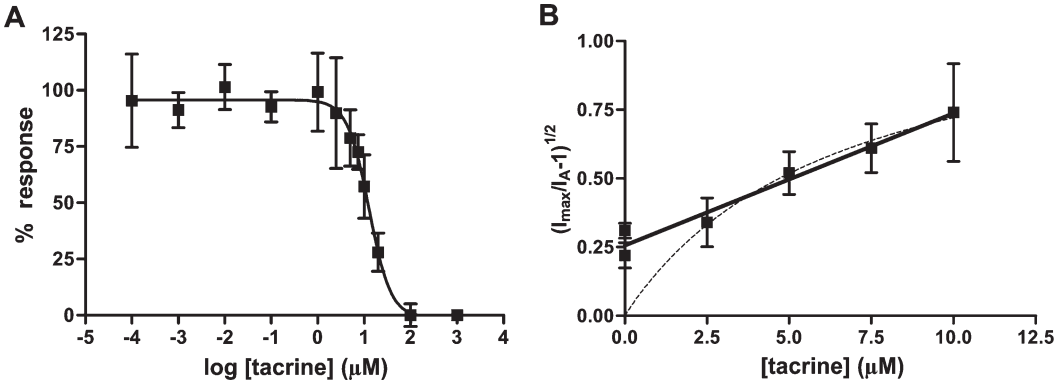

FIGURE 4: Characterization of the mechanism of inhibition of the rat $\alpha_3\beta_4$ nAChR by tacrine. Experimental conditions were as described in the Materials and Methods section, and all measurements were performed at a constant concentration of 300 μM nicotine and increasing tacrine concentrations. (A) The IC_{50} was determined as 13 ± 4 μM ($R^2 = 0.99$) with a Hill coefficient of -1.85 ± 0.96. (B) Curve fitting was carried out according to eq 4 by simulation of linear (solid line, in the case of competitive inhibitor) and nonlinear (dotted line, for a noncompetitive inhibitor) fitting. Linear fitting applied best for the data ($R^2 = 0.97$ and a slope of 0.048 ± 0.004 μM^{-1}) indicating a competitive mechanism. The constant for receptor inhibition by tacrine (K_I) was calculated to be 0.77 ± 0.01 μM. The simulation of a nonlinear fit gave a value for R^2 of 0.27.

cell surface receptors (shown by the dotted line) was calculated according to eq 1.

Whole-cell currents measured in voltage-clamped cells expressing rat $\alpha_3\beta_4$ nicotinic acetylcholine receptors depended on nicotine concentration. Current amplitudes obtained at different nicotine concentrations were normalized to those obtained with 300 μM (100%) to adjust for differences in receptor expression levels among cells and for small variations of the response amplitude over the time. A Hill plot reports the dependence of the concentration of open receptor channels on nicotine concentration with EC_{50} and n_H being 22 ± 4 μM and 1 ± 0.2, respectively (Figure 3A). The dissociation constant of the receptor site controlling channel opening (K_I) and the channel-opening equilibrium constant (Φ^{-1}) were 23 ± 0.2 μM and 4.3 ± 1.3, respectively, with I_{max} (mean maximal current when all channels are open) of 1733 pA (Figure 3B). The open squares and the dashed line in Figure 3A represent data obtained in the presence of a constant concentration (20 μM) of tacrine and will be discussed later.

The KXα3β4R2 cells expressing rat $\alpha_3\beta_4$ nicotinic acetylcholine receptors, which responded to stimulation with 300 μM nicotine with a large inward current, were also superfused with 100 pM, 1 nM, 10 nM, 100 nM, 1 μM, 100 μM, and 1 mM concentrations of tacrine. No ion currents were observed upon exposure to this drug, demonstrating that tacrine is not an agonist of $\alpha_3\beta_4$ nicotinic acetylcholine receptors (results not shown).

Inhibition of the $\alpha_3\beta_4$ nAChR by Tacrine. The dashed line in Figure 3A shows the dependence of nicotine-mediated response in KXα3β4R2 cells on nicotine concentration in the presence and absence of 20 μM tacrine. The dose−response curve is shifted to the right and to a higher EC_{50} value in the presence of tacrine, with no change in the maximal response. This result would be expected if tacrine was a competitive inhibitor of the $\alpha_3\beta_4$ nAChR but also if it acted as noncompetitive inhibitor binding mainly to the closed-channel forms. More quantitative approaches exist for differentiating between competitive and noncompetitive inhibitors than the shift in the dose−response curve, as illustrated in Figures 4 and 5.

Tacrine at 1−100 μM concentrations inhibited nicotine-mediated whole-cell currents when coapplied with nicotine. The Hill plot for tacrine-induced receptor inhibition is shown in Figure 4A. The IC_{50} value of the $\alpha_3\beta_4$ nAChR inhibition by tacrine was 13 ± 4 μM ($R^2 = 0.99$) with a Hill slope of -1.85 ± 0.97. The K_I value was calculated as 0.9 ± 0.4 μM by using eq 5 (Table 1).

In order to investigate the mechanisms by which tacrine inhibits the $\alpha_3\beta_4$ nAChR expressed on KXα3β4R2 cells, measurements were made at a constant concentration of nicotine (300 μM) and various concentrations of tacrine, and data were plotted in linear

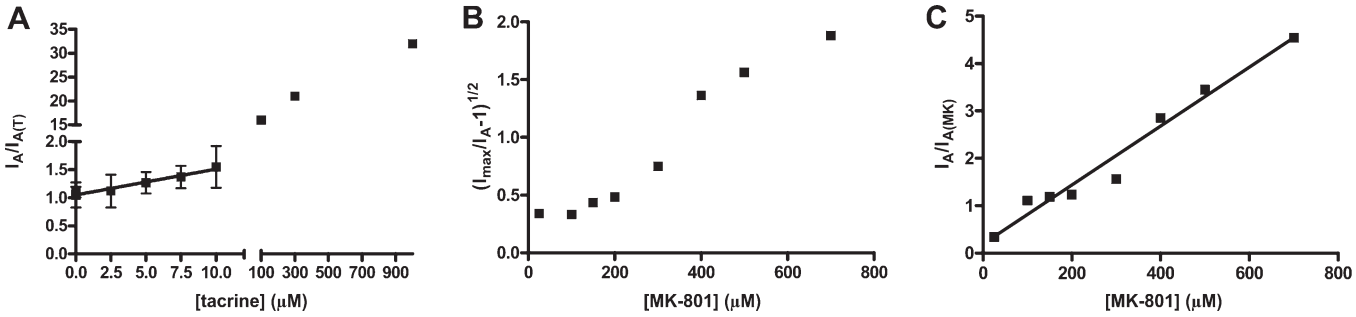

FIGURE 5: Inhibition studies of the $\alpha_3\beta_4$ nAChR inhibition in the presence of tacrine and MK-801. Maximum current amplitudes corrected for receptor desensitization were obtained in KXα3β4R2 cells with 300 μM nicotine in the absence or presence of the inhibitors tacrine and MK-801 at pH 7.4, room temperature, and a transmembrane voltage of −70 mV. (A) Inhibition of $\alpha_3\beta_4$ nAChR by tacrine. Only data points collected at a tacrine concentration of up to 10 μM were used for curve fitting. The slope of the fitted line was 0.05 ± 0.01 μM^{-1} with an intercept of 1.05 ± 0.07. Using eq 7, an apparent inhibition constant K_I of 23 ± 6 μM was calculated. Applying eq 8 and considering tacrine as a competitive inhibitor gave an inhibition constant (K_I) of 1.4 ± 0.4 μM. The breaks in the *x*- and *y*-axis ($I_A/I_{A(T)}$) are between 12 and 98 μM inhibitor concentration and 2 and 15, respectively. Note the deviation from linearity at higher concentrations of tacrine. (B) and (C) Inhibition of $\alpha_3\beta_4$ nAChRs by MK-801. The concentration of MK-801, a noncompetitive inhibitor, varied between 25 and 700 μM. For calculations, the average value for I_{max} of 1457 pA was used. For a noncompetitive inhibitor, a plot of $(I_{max}/I_{A-1})^{1/2}$ versus inhibitor concentration is not expected to be linear (eq 6). (C) The line has a slope of 0.006 ± 0.001 μM^{-1} and an intercept of 0.2 ± 0.4; using eq 7, an apparent inhibition constant K_I of 166 ± 29 μM was obtained. Note that the linear relation is still valid at higher inhibitor concentrations ($28K_I$).

Table 1: Inhibition Constants for Tacrine and MK-801

inhibitor	method for evaluation	figure	K_I (μM) competitive	K_I (μM) noncompetitive
tacrine	dose−response curve (eq 5)	4A	0.9 ± 0.4	
	$(I_{max}/I_A - 1)^{1/2}$ vs [tacrine] (eq 4)	4B	0.77 ± 0.01	
	$I_A/I_{A(T)}$ vs [tacrine] (eq 8)	5A	1.4 ± 0.4	
	$I_A/I_{A(T)}$ vs [tacrine] (eq 7)	5A		23 ± 6
MK-801	$I_A/I_{A(MK-801)}$ vs [MK-801] (eq 7)	5C		166 ± 29

(for a competitive inhibitor) and nonlinear (for a noncompetitive inhibitor) forms. The linear fit applied best for the data ($R^2 = 0.97$ and a slope of 0.048 ± 0.004), indicating a competitive mechanism. The channel-opening equilibrium constant (Φ^{-1}) was equal to 17.5 ± 0.5, as calculated from the intercept. The K_I value (inhibition constant) for tacrine at a nicotine concentration of 300 μM, calculated from the slope of the line, was 0.77 ± 0.01 μM (Table 1). In contrast, a $(I_{max}/I_A - 1)^{1/2}$ versus the inhibitor concentration plot for a noncompetitive inhibitor is expected to be nonlinear. Simulation of a nonlinear fitting gave a value for R^2 of 0.27 (Figure 4B).

The competitive mechanism by which tacrine inhibited $\alpha_3\beta_4$ nAChR expressed by KXα3β4R2 cells was confirmed by plotting the ratio of the current amplitudes obtained in cell-flow experiments, corrected for receptor desensitization, in the absence (I_A) and presence ($I_{A(T)}$) of inhibitor versus tacrine concentrations. The results were compared to those ones obtained in the presence of MK-801 ($I_A/I_{A(MK)}$), a noncompetitive inhibitor of the nAChRs (*5*). A linear relationship existed between $I_A/I_{A(I)}$ and the noncompetitive inhibitor over a wide concentration range (Figure 5C). In the case of a competitive inhibitor, however, the plot of the ratio of $I_A/I_{A(I)}$ versus competitive inhibitor concentration is expected to be linear only at low inhibitor concentrations, when $F_A(I/K_I)$ is small compared to $2F_A + F_{AL}$. F_A and F_{AL} represent the fraction of receptors in form A and AL, respectively. Figure 5A shows a plot of $I_A/I_{A(I)}$ versus tacrine concentration, at a constant concentration (300 μM) of nicotine according to eq 7. As expected for a competitive inhibitor, a linear relationship between $I_A/I_{A(I)}$ and tacrine concentration was obtained only at low inhibitor concentrations (0−10 μM). The values for F_A and F_{AL} were calculated using the K_I and Φ values obtained for nicotine only (Figure 2). The inhibition constant value obtained at low concentrations of the inhibitor tacrine and calculated by using eq 8 was 1.4 ± 0.4 μM. This value is in agreement with that obtained from the measurements shown in Figure 4B (Table 1). The curve fitted with eq 6 shows that a plot of $(I_{max}/I_A - 1)^{1/2}$ versus the inhibitor concentration is not linear, but it is proportional to the square root of inhibitor concentration times (Figure 5B).

In contrast, a plot of $I_A/I_{A(MK)}$ versus MK-801 concentration is linear over a wide concentration range of the inhibitor (Figure 5C). The results shown in this figure indicate that MK-801 is a noncompetitive inhibitor of the $\alpha_3\beta_4$ nAChR on KXα3β4R2 cells in the range of concentrations from 25 to 700 μM with a K_I value of 166 ± 29 μM. As expected for noncompetitive inhibitors (eq 7), a linear relationship between $I_A/I_{A(I)}$ and inhibitor concentration exists for a wide concentration range of MK-801.

As mentioned before, MK-801 is a well-known noncompetitive inhibitor of the nAChRs and should compete with TCP, another noncompetitive inhibitor of nAChRs (*6*), for the same binding sites. However, there should not be such competition between tacrine and TCP. To confirm this hypothesis and, once more, that tacrine inhibits the $\alpha_3\beta_4$ nAChR by competitive mechanisms, radioligand−receptor binding assays were performed. We investigated whether MK-801 and tacrine were able to displace [^{3}H]TCP from the $\alpha_3\beta_4$ nAChR expressed in KXα3β4R2 cells. [^{3}H]TCP was displaced from its binding sites on $\alpha_3\beta_4$ nAChR by MK-801, with an IC_{50} value of 71.0 ± 5.6 μM (Figure 6A), but not by tacrine (Figure 6B), even at high concentrations. These results indicate that TCP and MK-801 bind to the same site on the receptor, which is not occupied by tacrine, and corroborate our data showing that the latter inhibits the $\alpha_3\beta_4$ nAChR through a competitive mechanism. Similarly, representative current traces in Figure 6C demonstrate that tacrine and MK-801 bind to different sites and inhibit the $\alpha_3\beta_4$

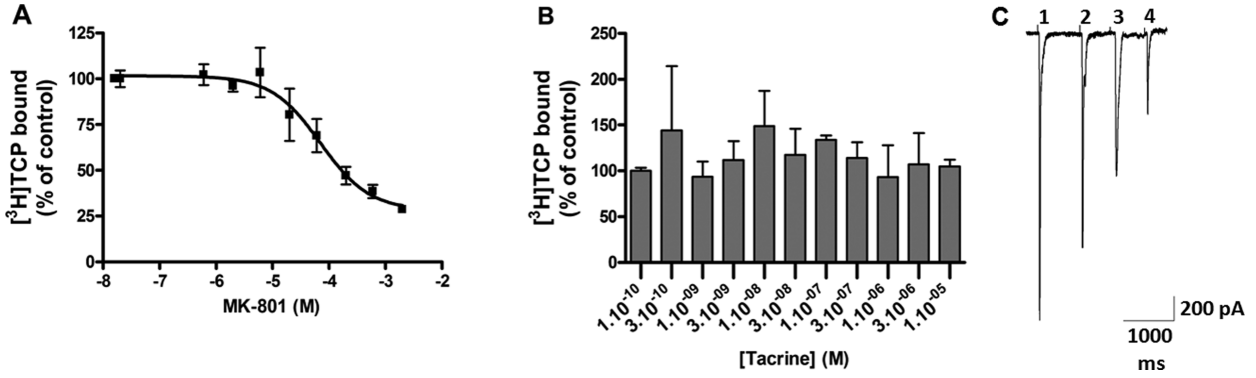

FIGURE 6: Competition of tacrine-receptor binding by TCP and MK-801. (A) Displacement of [^{3}H]TCP from $\alpha_3\beta_4$ nAChRs was studied in radioligand−receptor assays in the presence of increasing concentration of MK-801 and tacrine as detailed in the Materials and Methods section. Reported data were obtained in three independent experiments. (A) MK-801 displaced [^{3}H]TCP from its binding sites on receptor with IC_{50} equal to $71 \pm 5.6\,\mu$M. Note in (B) that tacrine did not interfere with [^{3}H]TCP receptor binding, even when employed at high concentrations. (C) Additive inhibition rates of nicotine-evoked whole-cell currents in the presence of MK-801 and tacrine: representative current recordings following application of 300 μM nicotine in the absence (1) and presence of 100 μM MK-801 (2), 20 μM tacrine (3), and together with 100 μM MK-801 and 20 μM tacrine (4). Data points for each drug were obtained with different cells, and percentage of inhibition was normalized to control responses in the absence of the respective inhibitor.

nAChR through additive effects and do not compete against each other.

DISCUSSION

Tacrine effects, an AChE inhibitor used for treatment of AD patients (*12*), on $\alpha_3\beta_4$ nAChR activity expressed in KXα3β4R2 cells were investigated utilizing a rapid chemical kinetic technique, the cell-flow technique with a millisecond time resolution (10−50 ms) (*23*). The current amplitudes due to the channel opening were determined by the patch-clamp technique (whole-cell configuration) and corrected for receptor desensitization that occurs while the receptors equilibrate with the ligand (nicotine solution with/without inhibitor) (*17*).

The minimum mechanism for nAChR activation was proposed by Katz and Thesleff and requires two molecules of agonist to bind to the receptor for channel opening (*24*). The receptor desensitization is initially rapid (millisecond) (*25*, *26*) and subsequently slow (*26*, *27*). The results shown here (Figure 2) indicate that $\alpha_3\beta_4$ nAChR desensitization is a complex process. Our data are in agreement with the literature mentioned before, according to which α characterizing the initial rapid desensitization process is at least 20 times greater than β, that characterizes the second desensitization process. In this work, α was around 120 times greater than β (Figure 2). Our results also indicate that only 2% of the receptors remained activated after the rapid desensitization process (Figure 2). Similar data were obtained from the organic ion flux measurements with receptor-containing electroplax membrane vesicles prepared from *Electrophorus electricus* (*28*).

First we investigated whether tacrine was an $\alpha_3\beta_4$ nAChR agonist, that is, whether it was able to bind to the receptor and induce the conformational alterations eventually leading to the channel opening and consequent cations influx. Cells responsive to superfusion of 300 μM nicotine with a large inward current, were stimulated with tacrine at a concentration ranging from 1 pM to 1 mM, and no ion currents were detected. Afterward, the same cells were exposed to 300 μM nicotine and there was a recovery of almost 100% of the initial measured response (data not shown), indicating that tacrine is not an agonist for these receptors, as well as it does not activate $\alpha_4\beta_2$ nAChR expressed on *Xenopus* oocytes (*29*).

The $\alpha_3\beta_4$ nAChR expressed on KXα3β4R2 cells was studied for its responsiveness to nicotine. Nicotine-induced ionic currents, whose amplitudes depended on ligand concentration, reached maximum values at an agonist concentration of 300 μM. At higher nicotine concentrations the amplitudes began to decrease (data not shown). This behavior, due to receptor block, has already been observed with other agonists, for instance, acetylcholine and carbamoylcholine (*16*, *29*). Therefore, nicotine is likely to bind to sites inside the channel and block the ion flux at high concentrations, when the ion channels are predominantly in the open state (*30*). The EC_{50} and n_H values determined as $22 \pm 4\,\mu$M and 1 ± 0.2, respectively, agree with previously published data. For example, Xiao and co-workers, utilizing $^{86}Rb^+$ efflux assays and the same cell line, obtained a EC_{50} value of $28.8 \pm 3.7\,\mu$M for the agonist nicotine (*16*). Our data also agree with the n_H values for $\alpha_2\beta_4$ and $\alpha_4\beta_4$ nAChR subtypes (*31*). According to our results, nicotine binds to $\alpha_3\beta_4$ nAChR with high affinity, which is implied from the K_I value ($K_d = 23 \pm 0.2\,\mu$M) calculated by using eq 3 (Figure 3). It is noteworthy that the EC_{50} and K_I values are almost the same. For the maximum current amplitude to be reached, it is necessary that the receptors are fully occupied in accordance with the proposed kinetic model. Following much the same investigation about the inhibition mechanisms of $\alpha_3\beta_4$ nAChR by cocaine, Hess and coworkers (*32*) determined a value of 3.3 ± 1 for the channel-opening equilibrium constant, Φ^{-1}. In our work, the calculated value was 4.3 ± 1.3, agreeing with the previously published data.

As already mentioned tacrine was not a nAChR agonist. However, tacrine strongly inhibited $\alpha_3\beta_4$ nAChR activity with an IC_{50} value of $13 \pm 4\,\mu$M (Figure 4A). The shift to the right and to higher EC_{50} value (from 22 to 73 μM) in the dose−response curve induced by tacrine, as illustrated in Figure 3A, was not sufficient to conclude that this compound is a competitive inhibitor, since receptor affinity for inhibitor also decreases as the agonist concentration increases in the presence of noncompetitive inhibitors binding preferentially to the closed-channel form. The experiments in Figures 4B and 5 differentiate between a noncompetitive, binding with higher affinity to closed-channel forms than to open-channel forms, and a competitive inhibitor.

The inhibition exerted by tacrine showed a competitive mechanism, giving a linear fitting when whole-cell currents in response to application of 300 μM nicotine $(I_{max}/I_A - 1)^{1/2}$ were plotted versus increasing tacrine concentrations (Figure 4B). The K_I values were calculated using eqs 4 and 5 and were nearly the

same (0.9 ± 0.4 μM versus 0.77 ± 0.01 μM, respectively) (Table 1).

In fact, there is much evidence that acetylcholine esterase inhibitors, i.e., physostigmine and galanthamine, to which also tacrine belongs, bind to nAChR agonist sites. In *Xenopus* oocytes expressing the fetal rat muscle nAChR, α-bungarotoxin, a competitive inhibitor of nAChRs, blocked currents observed in the presence of physostigmine, galanthamine, and their methyl derivatives, suggesting a competitive mechanism (*33*). Physostigmine-evoked macroscopic ion currents in insect neurons were blocked by competitive antagonists of nAChRs (*34*). Moreover, interaction of tacrine and nAChR agonist sites was also reported for other receptor subtypes. Svensson and Nordberg demonstrated that the nicotine-induced increase in number of $\alpha_2\beta_4$ nAChR in M10 cells was partially blocked when tacrine was applied together with nicotine, suggesting an interaction between these compound with the ACh binding site (*13*). In another work, the same authors demonstrated that the neuroprotective effect of tacrine in PC12 cells was blocked in the presence of the nicotinic competitive antagonist mecamylamine (*14*). Tacrine binding to agonist sites of muscle nAChR was also suggested (*35*). These authors demonstrated that, in spite of competition between tacrine and α-bungarotoxin, the main mechanism by which tacrine inhibits the muscle nAChR is by entering the channel and blocking it. One concludes, in the light of our results and the previously published work, tacrine inhibits the $\alpha_3\beta_4$ nAChR activity by a competitive mechanism.

Measurements with MK-801, a compound with anticonvulsive action (*36*), were performed to confirm the mechanism by which tacrine inhibits $\alpha_3\beta_4$ nAChR. The data presented in Figure 5 confirm conclusions that tacrine is a competitive antagonist. As expected for a competitive inhibitor (eq 8), a plot of $I_A/I_{A(I)}$ versus tacrine concentration gives a linear fitting only at low inhibitor concentrations. The K_I value determined for tacrine using eq 7 and considering it a noncompetitive inhibitor was 23 ± 6 μM (note the discrepancy between this value and the mentioned one before). On the other site, when tacrine was considered a competitive inhibitor, the K_I value given by eq 8 was 1.4 ± 0.4 μM, similar to values calculated using eqs 4 and 5 (Table 1). If we compare these data with those ones obtained with MK-801, we realize that, for this compound, a plot of $(I_{max}/I_A - 1)^{1/2}$ versus inhibitor concentration was not linear, whereas a plot of $I_A/I_{A(I)}$ versus inhibitor concentration was linear even at a wide MK-801 concentration range (Figure 5B,C). Subsequently, MK-801 is a noncompetitive inhibitor of $\alpha_3\beta_4$ nAChR in contrast to tacrine. As a matter of fact, MK-801 is one of most well characterized inhibitors of nicotinic receptors (*36*). Its K_I value for the $\alpha_3\beta_4$ subtype of nicotinic receptor, determined by Hess and co-workers, was 116 ± 16 μM, at a constant charbamoylcholine concentration of 3.3 mM (*32*), whereas ours was 166 ± 29 μM (Table 1), at a constant nicotine concentration of 300 μM.

We also confirmed the competitive mechanism for $\alpha_3\beta_4$ nAChR inhibition by tacrine employing radioligand binding assays. It was previously demonstrated that MK-801 and TCP, noncompetitive inhibitors of nAChRs (*6*, *36*), compete for the same sites on $\alpha_3\beta_4$ nAChR, whereas tacrine did not interfere with TCP receptor binding (Figure 6A,B). This experiment is consistent with that ones described earlier suggesting that tacrine is a competitive inhibitor. Moreover, current recordings were performed with nicotine alone and in the presence of MK-801 or tacrine and MK-801 and tacrine together. The representative current traces shown in Figure 6C indicate that the effects of MK-801 and tacrine on the $\alpha_3\beta_4$ nAChR were additive. Such result would be expected if MK-801 and tacrine inhibit the receptor through distinct mechanisms, not competing for the same binding sites.

It should be stressed, even though our data indicate a competitive mechanism for tacrine, that the compound does not necessarily compete for the agonist binding sites, as it has been shown that nicotine also binds to inhibitory sites on nicotinic receptors at the same concentrations at which it induces channel opening (*37*). In fact, several agonists may inhibit the receptors they activate (*30*, *38*, *39*). This inhibition may occur through either an increase in receptor desensitization rates resulting in a low probability of the receptor opening (a low Φ^{-1}) or by the capacity of the agonist to act as an open-channel blocker. For example, observations of cholinergic agonists inhibiting their receptors at higher concentrations, when the most of the receptors are in opened-channel form, suggest such mechanism of open-channel blockage. Receptor inhibition by agonists may occur alternatively via allosteric modulation, in which a noncompetitive inhibitor binds to a different site but interferes with agonist binding by inducing changes in the conformation of the receptor protein (*22*).

In summary, we do not exclude the possibility of tacrine binding to sites on the $\alpha_3\beta_4$ nAChR different from the agonist binding site. However, a direct interaction of tacrine with the agonist site of the receptor was suggested by increased $\alpha_3\beta_4$ nAChR desensitization rate in the presence of tacrine (data not shown). The channel-opening constant Φ^{-1} increases in the presence of tacrine by a factor of 4 (Figures 3B and 4B). The question is: How could an inhibitor increase the channel-opening probability (Φ^{-1})? The most obvious answer is that the inhibitor binds to the receptor molecule and stabilizes an inactive open-channel form of the receptor. Prince and co-workers (*35*) demonstrated that tacrine competes with α-bungarotoxin for agonist binding sites and functions like an open-channel blocker on muscle nAChR. It is plausible that more than one mechanism is involved in inhibition of the $\alpha_3\beta_4$ nAChR by tacrine.

Tacrine-evoked inhibition of the $\alpha_3\beta_4$ nAChR is of particular interest, given the use of this compound in treatment of Alzheimer's patients and, mainly, the roles played by the receptor in our organism. The $\alpha_3\beta_4$ nAChR is the main nicotinic receptor subtype found in the autonomic nervous system. Located in autonomic ganglia, it controls the release of catecholamines, such as norepinephrine and epinephrine, and consequently the sympathetic tonus of various tissues (*9*). The interaction between these catecholamines and their target receptors leads to an increase in vasoconstriction and blood pressure. On the other hand, inhibition of receptor activity shall result in vasodilatation and hypotension. In fact, $\alpha_3\beta_4$ nAChR inhibition by tacrine could account for, up to a certain point, the side effects shown by the drug, which include arterial hypotension such as also observed with anesthetics (*10*). However, tacrine-induced effects on the autonomic nervous system are not expected at therapeutic doses of the drug, as these concentrations do not inhibit α_7 and $\alpha_4\beta_2$ subtypes predominating in the CNS (*40*).

In summary, nanomolar and submicromolar concentrations of tacrine used for antagonizing acetylcholinesterase activity also result in inhibition of $\alpha_3\beta_4$ nAChR activity, by competing with nicotine for the agonist binding site and stabilizing a nonconducting open-channel receptor form.

ACKNOWLEDGMENT

We thank Prof. Yingxian Xiao (Department of Pharmacology, Georgetown University, Washington, DC) for the gift of the KXα3β4R2 cell line expressing the rat neuronal $\alpha_3\beta_4$ nAChR.

REFERENCES

1. Sine, S. M., and Engel, A. G. (2006) Recent advances in Cys-loop receptor structure and function. *Nature 440*, 448–455.
2. Jensen, A. A., Frolund, B., Liljefors, T., and Krogsgaard Larsen, P. (2005) Neuronal nicotinic acetylcholine receptors: structural revelations, target identifications and therapeutic inspirations. *J. Med. Chem. 48*, 4705–4745.
3. Niu, L., and Hess, G. P. (1993) An acetylcholine receptor regulatory site in BC3H1 cells: characterized by laser-pulse photolysis in the microsecond-to-millisecond time region. *Biochemistry 32*, 3831–3835.
4. Gentry, C. L., and Lukas, R. J. (2001) Local anesthetics noncompetitively inhibit function of four distinct nicotinic acetylcholine receptor subtypes. *J. Pharmacol. Exp. Ther. 299*, 1038–1048.
5. Hess, G. P., Ulrich, H., Breitinger, H. G., Niu, L., Gameiro, A. M., Grewer, C., Srivastava, S., Ippolito, J. E., Lee, S. M., Jayaraman, V., and Coombs, S. E. (2000) Mechanism-based discovery of ligands that counteract inhibition of the nicotinic acetylcholine receptor by cocaine and MK-801. *Proc. Natl. Acad. Sci. U.S.A. 25*, 13895–13900.
6. Ulrich, H., Ippolito, J. E., Pagán, O. R., Eterović, V. A., Hann, R. M., Shi, H., Lis, J. T., Eldefrawi, M. E., and Hess, G. P. (1998) In vitro selection of RNA molecules that displace cocaine from the membrane-bound nicotinic acetylcholine receptor. *Proc. Natl. Acad. Sci. U.S.A. 24*, 14051–14056.
7. Ulrich, H., Akk, G., Nery, A. A., Trujillo, C. A., Rodriguez, A. D., and Eterović, V. A. (2008) Mode of cembranoid action on embryonic muscle acetylcholine receptor. *J. Neurosci. Res. 86*, 93–107.
8. Ferchmin, P. A., Pagán, O. R., Ulrich, H., Szeto, A. C., Hann, R. M., and Eterović, V. A. (2009) Actions of octocoral and tobacco cembranoids on nicotinic receptors. *Toxicon 54*, 1174–1182.
9. Court, J., Martin Ruiz, C., Graham, A., and Perry, E. (2000) Nicotinic receptors in human brain: topography and pathology. *J. Chem. Neuroanat. 20*, 281–298.
10. Tassonyi, E., Charpantier, E., Muller, D., Dumont, L., and Bertrand, D. (2002) The role of nicotinic acetylcholine receptors in the mechanisms of anesthesia. *Brain Res. Bull. 57*, 133–150.
11. Taraschenko, O. D., Panchal, V., Maisonneuve, I. M., and Glick, S. D. (2005) Is antagonism of alpha3beta4 nicotinic receptors a strategy to reduce morphine dependence? *Eur. J. Pharmacol. 513*, 207–218.
12. Munoz Ruiz, R. L., Garcia Palomero, E., Dorronsoro, I., Del Monte Millan, M., Valenzuela, R., Usan, P., De Austria, C., Bartolini, M., Andrisano, V., Bidon Chanal, A., Orozco, M., Luque, F. J., Medina, M., and Martinez, A. (2005) Design, synthesis, and biological evaluation of dual binding site acetylcholinesterase inhibitors: new disease-modifying agents for Alzheimer's disease. *J. Med. Chem. 48*, 7223–7233.
13. Svensson, A., and Nordberg, A. (1996) Tacrine interacts with an allosteric activator site on alpha 4 beta 2 nAChRs in M10 cells. *Neuroreport 7*, 2201–2205.
14. Svensson, A. L., and Nordberg, A. (1998) Tacrine and donepezil attenuate the neurotoxic effect of A beta(25−35) in rat PC12 cells. *Neuroreport 9*, 1519–1522.
15. Krishtal, O. A., and Pidoplichko, V. I. (1980) A receptor for protons in the nerve cell membrane. *Neuroscience 5*, 2325–2327.
16. Xiao, Y., Meyer, E. L., Thompson, J. M., Surin, A., Wroblewski, J., and Kellar, K. J. (1998) Rat $\alpha_3\beta_4$ subtype of neuronal nicotinic acetylcholine receptor stably expressed in a transfected cell line: pharmacology of ligand binding and function. *Mol. Pharm. 54*, 322–333.
17. Udgaonkar, J. B., and Hess, G. P. (1987) Chemical kinetic measurements of a mammalian acetylcholine receptor by a fast-reaction technique. *Proc. Natl. Acad. Sci. U.S.A. 84*, 8758–8762.
18. Hamill, O. P., Marty, A., Neher, E., Sakmannn, B., and Sigworth, F. J. (1981) Improved patch-clamp techniques for high-resolution current recording from cells and cell-free membrane patches. *Pfluegers Arch. 391*, 85–100.
19. Cash, D. J., and Hess, G. P. (1980) Molecular mechanism of acetylcholine receptor-controlled ion translocation across cell membranes. *Proc. Natl. Acad. Sci. U.S.A. 77*, 842–6.
20. Trujillo, C. A., Nery, A. A., Martins, A. H., Majumder, P., Gonzalez, F. A., and Ulrich, H. (2006) Inhibition mechanism of the recombinant rat P2X(2) receptor in glial cells by suramin and TNP-ATP. *Biochemistry 45*, 224–233.
21. Cheng, Y., and Prusoff, W. H. (1973) Relationship between the inhibition constant (K1) and the concentration of inhibitor which causes 50% inhibition (I50) of an enzymatic reaction. *Biochem. Pharmacol. 22*, 3099–3108.
22. Breitinger, H. G., Geetha, N., and Hess, G. P. (2001) Inhibition of the serotonin 5-HT3 receptor by nicotine, cocaine, and fluoxetine investigated by rapid chemical kinetic technique. *Biochemistry 40*, 8419–8429.
23. Ulrich, H., and Gameiro, A. M. (2001) Aptamers as tools to study dysfunction in the neuronal system. *Curr. Med. Chem. 1*, 125–132.
24. Katz, B., and Thesleff, S. (1957) A study of the desensitization produced by acetylcholine at the motor end-plate. *J. Physiol. 138*, 63–80.
25. Hess, G. P., Cash, D. J., and Aoshima, H. (1979) Acetylcholine receptor-controlled ion fluxes in membrane vesicles investigated by fast reaction techniques. *Nature 282*, 329–331.
26. Sakmann, B., Patlak, J., and Neher, E. (1980) Single acetylcholine-activated channels show burst-kinetics in presence of desensitizing concentrations of agonist. *Nature 286*, 71–73.
27. Walker, J. W., McNamee, M. G., Pasquale, E., Cash, D. J., and Hess, G. P. (1981) Acetylcholine receptor inactivation in *Torpedo californica* electroplax membrane vesicles. Detection of two processes in the millisecond and second time regions. *Biochem. Biophys. Res. Commun. 100*, 86–90.
28. Aoshima, H., Cash, D. J., and Hess, G. P. (1981) Mechanism of inactivation (desensitization) of acetylcholine receptor. Investigations by fast reaction techniques with membrane vesicles. *Biochemistry 20*, 3467–3474.
29. Smulders, C. J., Zwart, R., Bermudez, I., Van Kleef, R. G., Groot Kormelink, P. J., and Vijverberg, H. P. (2005) Cholinergic drugs potentiate human nicotinic alpha4beta2 acetylcholine receptors by a competitive mechanism. *Eur. J. Pharmacol. 509*, 97–108.
30. Sine, S. M., and Steinbach, J. H. (0000) Agonists block currents through acetylcholine receptor channels. *Biophys. J. 46*, 277–283.
31. Stauderman, K. A., Mahaffy, L. S., Akong, M., Veliçelebi, G., Chavez Noriega, L. E., Crona, J. H., Johnson, E. C., Elliott, K. J., Gillespie, A., Reid, R. T., Adams, P., Harpold, M. M., and Corey Naeve, J. (1998) Characterization of human recombinant neuronal nicotinic acetylcholine receptor subunit combinations alpha2beta4, alpha3beta4 and alpha4beta4 stably expressed in HEK293 cells. *J. Pharmacol. Exp. Ther. 284*, 777–789.
32. Krivoshein, A. V., and Hess, G. P. (2004) Mechanism-based approach to the successful prevention of cocaine inhibition of the neuronal (alpha 3 beta 4) nicotinic acetylcholine receptor. *Biochemistry 43*, 481–489.
33. Cooper, J. C., Gutbrod, O., Witzemann, V., and Methfessel, C. (1996) Pharmacology of the nicotinic acetylcholine receptor from fetal rat muscle expressed in Xenopus oocytes. *Eur. J. Pharmacol. 309*, 287–298.
34. Van Den Beukel, I., Van Kleff, R. G., Zwart, R., and Oorgiesen, M. (1998) Physostigmine and acetylcholine differentially activate nicotinic receptor subpopulations in Locusta migratoria neurons. *Brain Res. 789*, 263–273.
35. Prince, R. J., Pennington, R. A., and Sine, S. M. (2002) Mechanism of tacrine block at adult human muscle nicotinic acetylcholine receptors. *J. Gen. Physiol. 120*, 369–393.
36. Grewer, C., and Hess, G. P. (1999) On the mechanism of inhibition of the nicotinic acetylcholine receptor by the anticonvulsant MK-801 investigated by laser-pulse photolysis in the microsecond-to-millisecond time region. *Biochemistry 38*, 7837–7846.
37. Tonner, P. H., Wood, S. C., and Miller, K. W. (1992) Can nicotine self-inhibition account for its low efficacy at the nicotinic acetylcholine receptor from Torpedo? *Mol. Pharmacol. 42*, 890–897.
38. Forman, S. A., Firestone, L. L., and Miller, K. W. (1987) Is agonist self-inhibition at the nicotinic acetylcholine receptor a nonspecific action? *Biochemistry 26*, 2807–2814.
39. Ogden, D. C., and Colquhoun, D. (1985) Ion channel block by acetylcholine, carbachol and suberyldicholine at the frog neuromuscular junction. *Proc. R. Soc. London, Ser. B: Biol. Sci. 225*, 329–355.
40. Picciotto, M. R., Caldarone, B. J., Brubzell, D. H., Zachariou, V., Stevens, T. R., and King, S. L. (2001) Neuronal nicotinic acetylcholine receptor subunit knockout mice: physiological and behavioral phenotypes and possible clinical implications. *Pharmacol. Ther. 92*, 89–108.